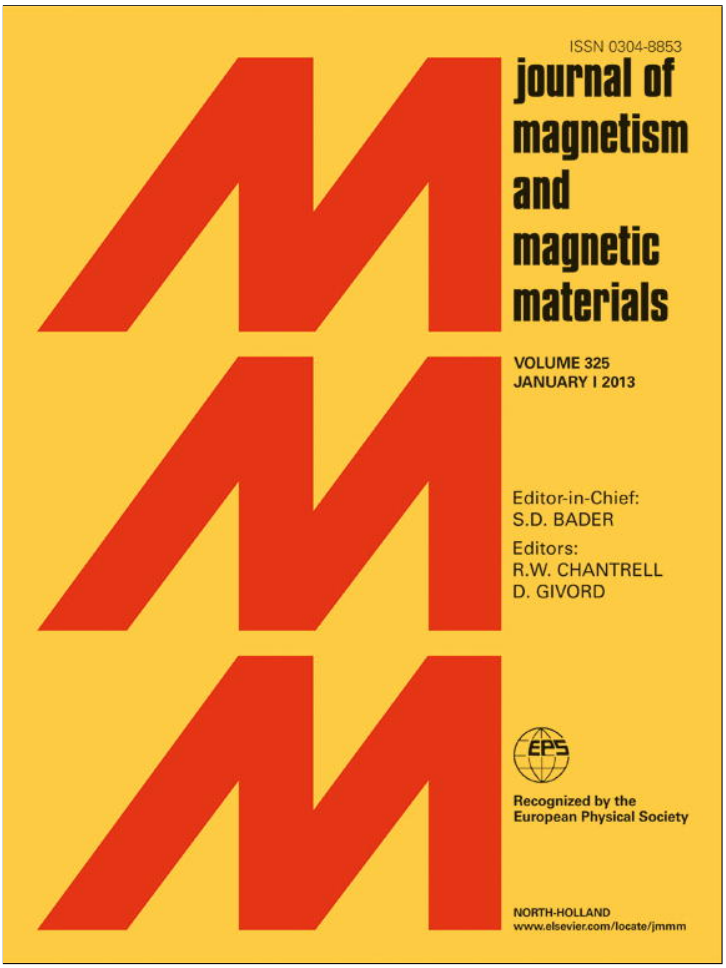

Journal of Magnetism and Magnetic Materials 325 (2013) 63–68

Contents lists available at SciVerse ScienceDirect

Journal of Magnetism and Magnetic Materials

journal homepage: www.elsevier.com/locate/jmmm

Synthesis and electromagnetic properties of U-type hexaferrites $Ba_4B_2Fe_{36}O_{60}$ (B: Co, Ni, Cu)

S.R. Shannigrahi [a,*], W.Q. Au [b], V. Suresh Kumar [b], L. Liu [c], Z.H. Yang [c], C. Cheng [b], C.K.I. Tan [a], R.V. Ramanujan [b]

[a] Institute of Materials Research and Engineering, A*STAR (Agency for Science Technology and Research), 3 Research Link, Singapore 117602, Singapore
[b] School of Materials Science and Engineering, Nanyang Technological University, Nanyang Avenue 50, Singapore 639798, Singapore
[c] Temasek Laboratories, National University of Singapore, Singapore 117508, Singapore

ARTICLE INFO

Article history:
Received 25 June 2012
Received in revised form
2 August 2012
Available online 24 August 2012

Keywords:
U-type hexaferrite
Solid state sintering
Microwave absorption

ABSTRACT

Polycrystalline samples of U-type hexaferrites $Ba_4B_2Fe_{36}O_{60}$ (B: Co, Ni and Cu) were synthesized using a modified solid state reaction technique. The sintered hexaferrites were tested for their crystalline quality using x-ray diffraction technique and their magnetic properties using the Physical Property Measurement System (PPMS). The individual ferrites were further used as fillers to prepare composites using a polyethylene matrix. The composites were tested for their complex permittivity and permeability spectra and finally reflection loss spectra were derived from these results. Among the studied composites, lowest and highest values of saturation magnetization were 25 and 35 emu/g, respectively, for the Cu doped hexaferrites and the Co doped hexaferrites. All the studied composites demonstrated microwave absorption property, which was tunable by manipulating the sample thickness. Co-doped composites offered the highest absorption (~98%) and were found the most suitable to suppress electromagnetic interference.

1. Introduction

Ferrites are very important class of materials for their high magnetic permeability, low core loss and soft magnetic nature [1–3]. This allows them to be useful in various applications such as electronic devices or components as well as magnetic materials in microwave applications [4–6]. Hexaferrites are ferrites with the complex crystal structure $AO–Fe_2O_3–BO$, where A=Ba, Sr, Ca, La and B=bivalent transition metal. The different stable phases of hexaferrites, in the increasing order of complexity are M, Y, W, Z, X and U. Out of these, the U-type hexaferrite $Ba_4B_2Fe_{36}O_{60}$ has the most complex crystal structure and the largest unit cell size. There are not many reports available on the magnetic characterization of the U-type hexaferrites. One of the U-type hexaferrite compounds, $Sr_4Co_2Fe_{36}O_{60}$, is known to exhibit a ferrimagnetic ordering below temperatures as high as 690 K [4]. The temperature dependent magnetization along with the neutron diffraction measurements reveals that the Neel transition occurs at two different temperatures 690 K and 350 K. Moreover, U-type hexaferrites are more useful for their suitability in wide frequency applications [1–7]. The hexagonal structure of hexaferrites allows having extremely high intrinsic magnetocrystalline anisotropy [2–4]. This gives them a unique combination of dielectric and magnetic properties at high frequencies and are suitable for microwave frequency region [2,3] due to their uni-axial magnetic anisotropy [4–6].

Electromagnetic interference (EMI) causes malfunction of wireless communication systems and it is essential to develop EMI shielding/absorbing materials applicable for a wide frequency region. However, to generate industrial attention, the preferred material to be cheap, light weight and corrosion free [3]. To achieve these features, hexaferrite filler and polymer matrix based composites would be the best choice as these could be of very light weight, low cost and have non-corrosive nature. Keeping these features in mind, this work focuses on the synthesis of U-type hexaferrites with a chemical formula of $Ba_4B_2Fe_{36}O_{60}$, where B=Co, Ni, and Cu and employing these as fillers in a polyethylene matrix to prepare composites for EMI shielding applications [8–12]. Because of the structural complexity the U-type hexaferrites are difficult to prepare using the normal solid state reaction process. Moreover, most solid state ceramic processings involve long processing times (typically 24 h of ball milling), followed by calcination and sintering, which consume a lot of resources and the overall process is too costly to be adopted by industries. Hence, a modified solid state reaction process was adopted by incorporating an additional step of

* Corresponding author. Tel.: +65 68748299; fax: +65 68720785.
E-mail address: santi-s@imre.a-star.edu.sg (S.R. Shannigrahi).

0304-8853/$ - see front matter © 2012 Elsevier B.V. All rights reserved.
http://dx.doi.org/10.1016/j.jmmm.2012.08.019

ultrasonic processing during the solid state reaction process for greater homogeneity in the mixture; this resulted in lower calcination and sintering temperatures [13].

2. Experimental details

U-type hexaferrites with the general formula $Ba_4B_2Fe_{36}O_{60}$ (B: Co, Ni and Cu; hereafter, U-Co, U-Ni and U-Cu) were prepared using $BaCO_3$ (99.95%), Fe_2O_3 (99.95%), CoO (99.9%), NiO (99.9%) and CuO (99.9%) as raw starting materials. The raw starting materials were first stoichiometrically weighed and mixed followed by ultrasonication for 30 min with ultrasonic irradiation using a direct-immersion titanium horn (Sonics VCX500, 20 kHz, 500 W, Sonics & Materials Inc., Newtown, CT). After the ultrasonication process, the slurry was dried and crushed again followed by calcination at 1100 °C in air ambient for 6 h with cooling/heating rate of 10 °C/min. The calcined powders were ball-milled in ethanol medium for 4 h and mixed with 4 wt% polyvinyl butyral (PVB) as a binder and were pressed into pellets with a diameter of 15 mm using a uniaxial cold hydraulic press (pressure of 10 MPa). The pellets were sintered at an optimized temperature of 1275 °C for 6 h after several trials. The crystal structures of the samples were determined using x-ray diffraction (XRD; D8 ADVANCED, Bruker AXS GmbH, Karlsruhe, Germany). To produce a composite, polyethylene was selected as matrix and the sintered ferrite powders were used as fillers of 60 wt%. The mixture was added to a melt mixing compounding machine at a temperature of 150 °C, which mixed the fillers evenly within the polymer matrix. The individual fillers as well as their composites were further tested for magnetic properties using the Physical Property Measurement System (PPMS; Quantum Design). The complex permittivity ($\varepsilon_r=\varepsilon'-j\varepsilon''$) and permeability ($\mu_r=\mu'-j\mu''$) values of the composites in the frequency range of 1 MHz–1 GHz were measured by using an Agilent VNA (Vector Network Analyzer) HP8722D with a reflection-through-line calibration using a set of 14 mm coaxial air-line with length of 59.96 mm. The investigated samples used for microwave studies were toroid shaped with an outer diameter of 14 mm, inner diameter of 7 mm and thickness of about 2 mm. The electromagnetic (EM) parameters (ε', ε'', μ' and μ'') were then calculated by the materials measurement software. Using these EM parameters, the reflection loss (R_L) was calculated and microwave absorbing properties were determined in the given frequency range and absorber thickness according to the following equations:

$$\frac{Z_{in}}{Z_0}=\sqrt{\frac{\mu_r}{\varepsilon_r}}tanh\left[j\frac{2\pi ft}{c}\sqrt{\mu_r\varepsilon_r}\right] \quad (1)$$

$$R_L(dB)=20log_{10}\left|\frac{Z_{in}-Z_0}{Z_{in}+Z_0}\right| \quad (2)$$

where Z_{in} is impedance of the composites backed by a ground plane, Z_0 is the intrinsic impedance of free space, c is the velocity of light in free space, t is the thickness of the attenuation material, and f is the frequency of the incident EM wave.

3. Results and discussion

Fig. 1 presents the XRD pattern of the sintered hexaferrites. The peaks at around 24°, 30–38°, 40–43°, 55–58° and 64° represent the signature of the U-type hexaferrites. No noticeable amounts of unknown peaks were observed in the studied systems. This shows that the prepared hexaferrites are phase pure in nature [3,5,6,14]. It was further observed that the duration of ultrasonic agitation affects the phase purity of U-type hexaferrite. The 30 min duration of ultrasonic agitation was found to be the best duration. U-type hexaferrite originates from the combination of 2M-type and 1Y-type structure [5,6,15]. If the sintering or calcinations temperature is too high, Z-type will be formed instead of M-type or Y-type and there will be lesser reaction between M and Y types to form U-type, resulting in a multiphase hexaferrite structure. Therefore, temperature must be optimized to prevent the formation of Z-type hexaferrites and possible low sintering temperature to improve the phase purity of the sample by reducing both unwanted phase of Fe and Z-type hexaferrite. This shows that single phase U-Co is obtained at calcination temperature of 1100 °C as well. Sintering condition was optimized using 1275 °C for 6 h. The sintering temperature above 1275 °C results in the formation of Fe phases and Z-type hexaferrite.

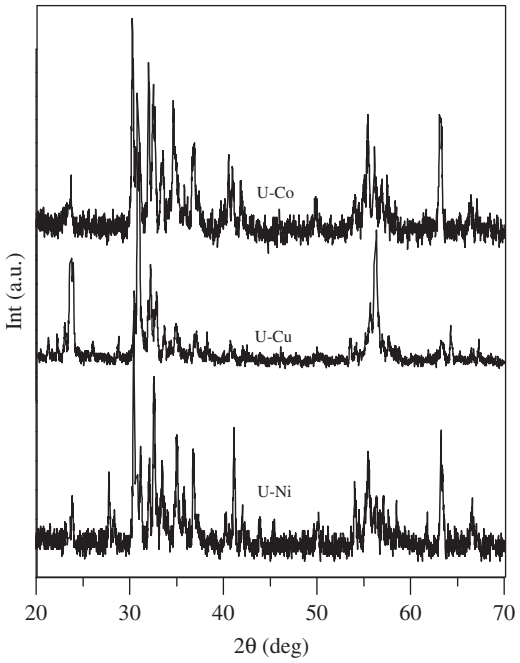

Fig. 1. XRD patterns of the $Ba_4X_2Fe_{36}O_{60}$ (X = Co, Ni and Cu) hexaferrites sintered at 1275 °C for 6 h.

The field dependent magnetization curves for $Ba_4B_2Fe_{36}O_{60}$ (B = Co, Ni and Cu) and the composites were measured between the fields of −2 to 2 T at selected temperatures using Vibrating Sample Magnetometer integrated with Quantum Design PPMS. The intrinsic magnetic parameters such as saturation magnetization (M_s), inhomogeneity constant (A), magnetocrystalline anisotropy field (H_a) and magnetocrystalline anisotropy constant (K_1) have been determined from the numerical analysis of the measured magnetization curves based on the law of approach to saturation.

$$M=M_s\left(1-\frac{A}{H}-\frac{B}{H^2}-\frac{C}{H^3}\right) \quad (3)$$

where H is the applied field and M_s is the saturation magnetization. The parameter A is related to the existence of inhomogeneities in the material, and the other two parameters B and C are related to the magnetocrystalline anisotropy field.

The field dependent magnetization M–H curves for $Ba_4B_2Fe_{36}O_{60}$ (B = Co, Ni and Cu) measured between the fields −2 T and 2 T at temperatures 4 K, 50 K, 100 K, 150 K, 200 K and 300 K are shown in Fig. 2. It is very clear that all the three samples do not exhibit considerable field hysteresis even at temperatures as low as 4 K. The Co substituted sample shows the highest value of magnetization at 4 K under the field of 2 T compared to other two samples. We can also observe that unlike Co and Ni (shown in the

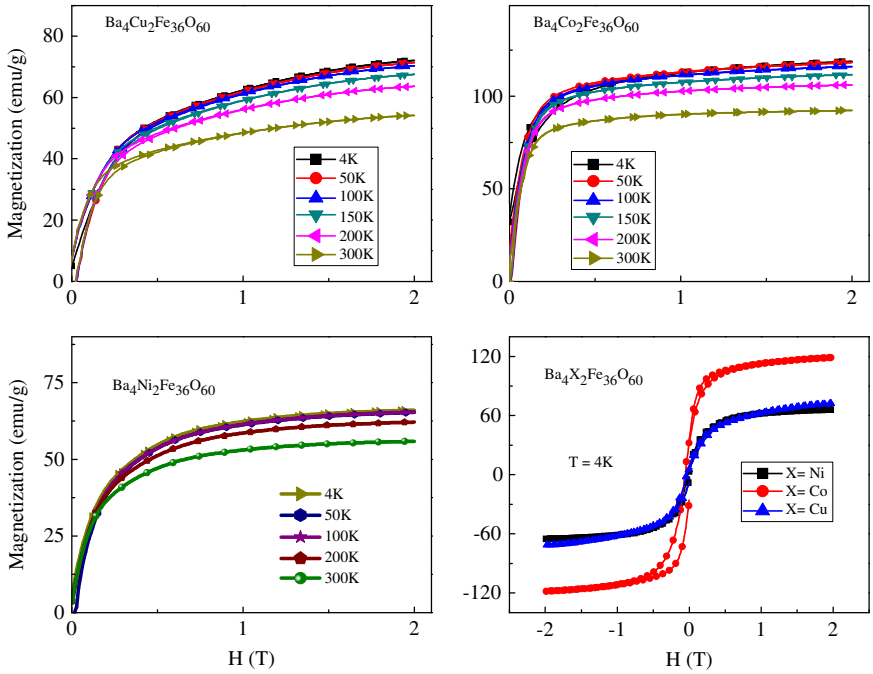

Fig. 2. Field dependent magnetization for the $Ba_4X_2Fe_{36}O_{60}$ (X═Co, Ni and Cu) hexaferrites measured at selected temperatures.

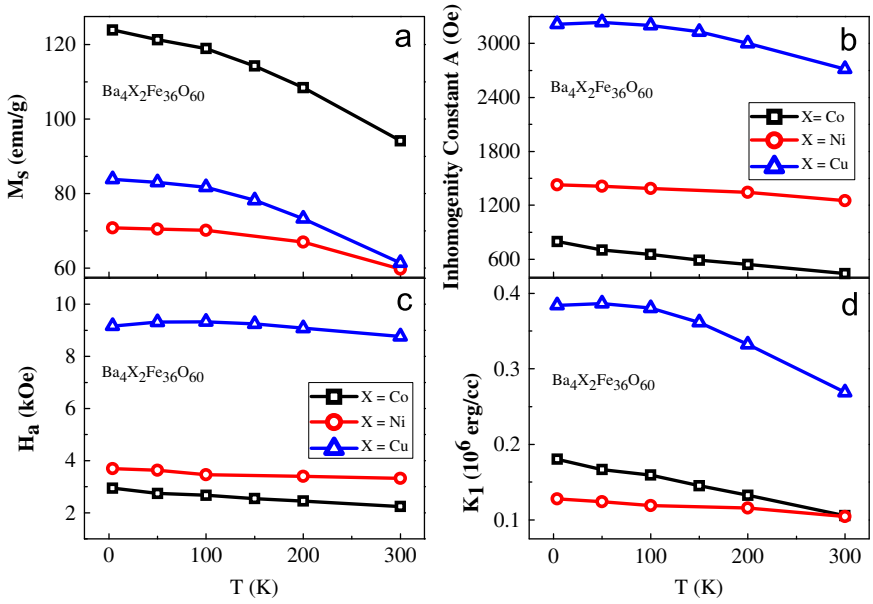

Fig. 3. Temperature dependence of (a) saturation magnetization (M_s), (b) inhomogeneity constant (A), (c) magnetocrystalline anisotropy field (H_a) and (d) magnetocrystalline anisotropy constant (K_1) for the $Ba_4X_2Fe_{36}O_{60}$ (X═Co, Ni and Cu) hexaferrites.

inset) the high field region ($H\sim2$ T) of magnetization for Cu does not show a complete saturation behavior and perhaps fields more than 2 T are required to completely saturate the sample. This behavior is expected as Cu is diamagnetic, while Co and Ni are ferromagnetic elements. From these field dependent magnetization curves we can also infer that the magnetic transition temperature is well above 300 K.

The temperature dependent saturation magnetization determined for $Ba_4B_2Fe_{36}O_{60}$ (B═Co, Ni and Cu) is shown in Fig. 3(a). The U-Co sample exhibits the highest value of 123.87 emu/g for M_s at 4 K, which is higher than those of $Sr_4Co_2Fe_{36}O_{60}$ and $Ba_4Co_2Fe_{36}O_{60}$ fibers reported earlier [4]. The values of M_s for all the samples decrease with temperature, which is in agreement with the fact that the thermal energy dominates over the magnetic energy as we proceed to higher temperatures. The decrease in M_s with temperature is very small between the temperatures 4 K and 50 K, monotonic between 50 K and 200 K and rapidly changing between 200 K and 300 K. The inhomogeneity constant A determined from the fits to Eq. (3) as a function of temperature is shown in Fig. 3(b). This constant actually represents the inhomogeneities present in the crystal and also the mobility of magnetization. The higher the value of A, the more difficult it is to magnetize the sample. The values of A shown in Fig. 3(b) for U-Cu, U-Ni and U-Co very well support that its relatively easier to magnetize U-Co sample than U-Ni and U-Cu.

Barium ferrites with hexagonal structure are known to have two types of anisotropy, c-axis anisotropy associated with the easy direction of magnetization along c-axis and easy plane

anisotropy corresponding to the easy direction of magnetization along *c*-plane. In the present case, the magnetocrystalline anisotropy determined can be the resultant of these two. The anisotropy field H_a determined from the law of approach to saturation as a function of temperature for the three samples is shown in Fig. 3(c). In eq. (3) the terms B/H^2 and C/H^3 are related to the magnetocrystalline anisotropy. The values of B and C are determined from the polynomial fit to the M vs $1/H$ experimental data in the high field region. As these samples possess hexagonal symmetry the magnetocrystalline anisotropy filed (H_a) can be expressed in terms of B and C using the following equations:

$$B = -\frac{1}{15}H_a^2 \tag{4}$$

$$C = \frac{2}{105}H_a^3 \tag{5}$$

And further H_a can be related to the first order magnetocrystalline anisotropy constant K_1:

$$H_a = \frac{2K_1}{M_s} \tag{6}$$

The temperature dependent value of K_1 estimated using Eq. (6) for all the samples is shown in Fig. 3(d). The magnetocrystalline anisotropy field and so also the magnetocrystalline anisotropy constant have dominant values for X=Cu sample and decrease with increasing temperature.

The field dependent magnetization for composites (60 wt%) for $Ba_4X_2Fe_{36}O_{60}$ (X=Co, Cu and Ni) recorded at 300 K is shown in Fig. 4. Surprisingly Cu and Ni seem to have the same effect in the composite form, even though X=Ni exhibited higher magnetization at 300 K. The Co sample in the composite form has less magnetization compared to the other two samples unlike in the pure form.

Figs. 5, 6 and 7 show the frequency variation of real and imaginary parts of complex permittivity ($\varepsilon_r=\varepsilon'-j\varepsilon''$) and permeability ($\mu_r=\mu'-j\mu''$) for U-Co, U-Ni and U-Cu based composites respectively at room temperature. In the coaxial line measurement method, when the wavelength of propagation wave is twice of the length of the fixture, there are resonances which result in spikes in the measured permittivity and permeability. These resonances are not related to the relaxation, or noise. It is the system error, which could be trimmed. The average values of real part of dielectric constant (ε') are almost constant; however, the

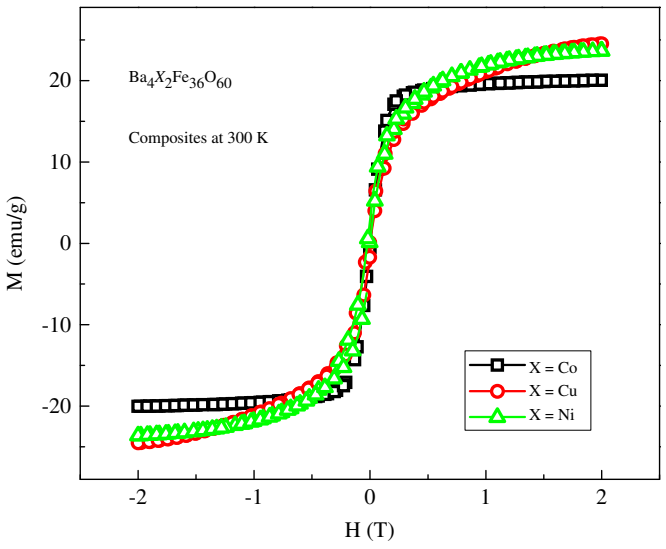

Fig. 4. Field dependent magnetization for composites of the $Ba_4X_2Fe_{36}O_{60}$ (X=Co, Ni and Cu) measured at 300 K.

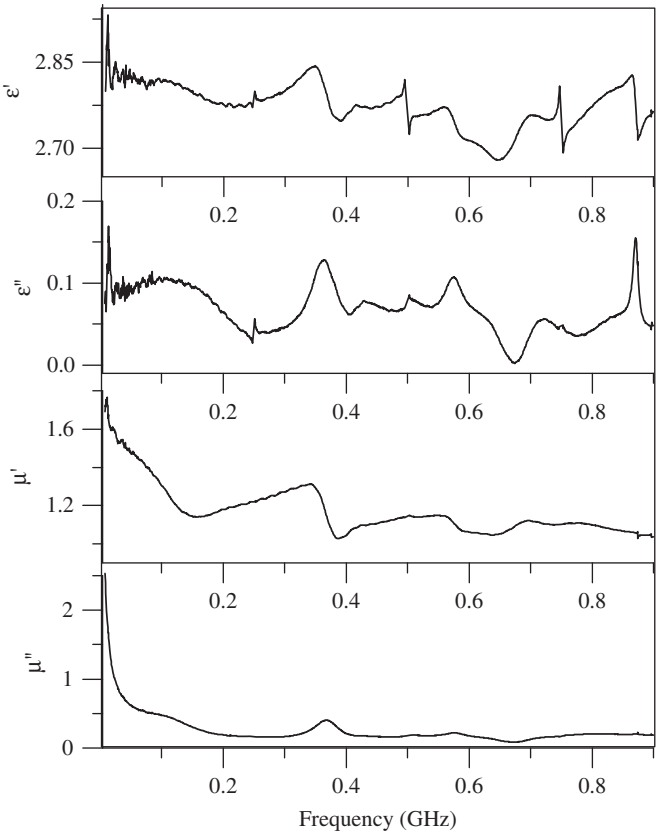

Fig. 5. Frequency variation of dielectric permittivity and magnetic permeability spectra of the $Ba_4Co_2Fe_{36}O_{60}$ based composites.

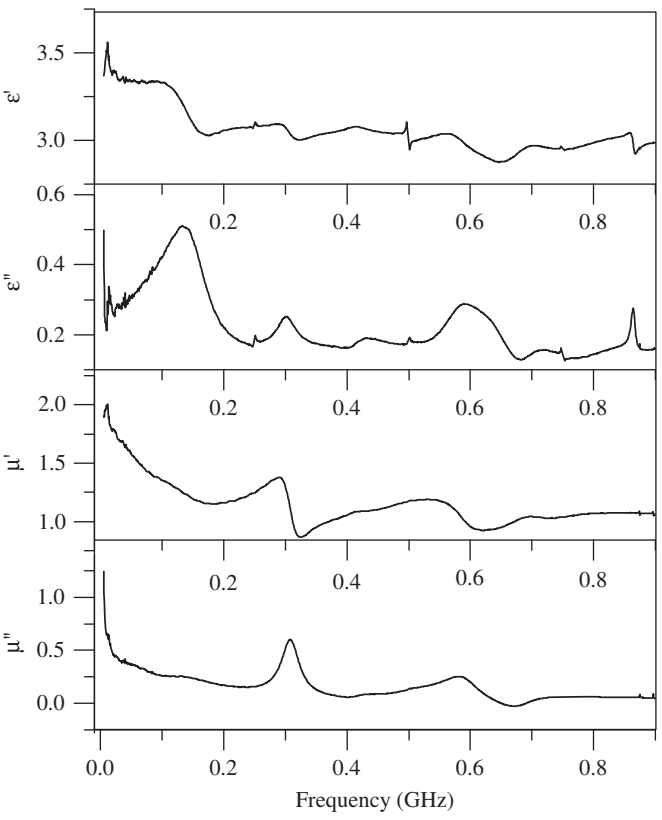

Fig. 6. Frequency variation of dielectric permittivity and magnetic permeability spectra of the $Ba_4Ni_2Fe_{36}O_{60}$ based composites.

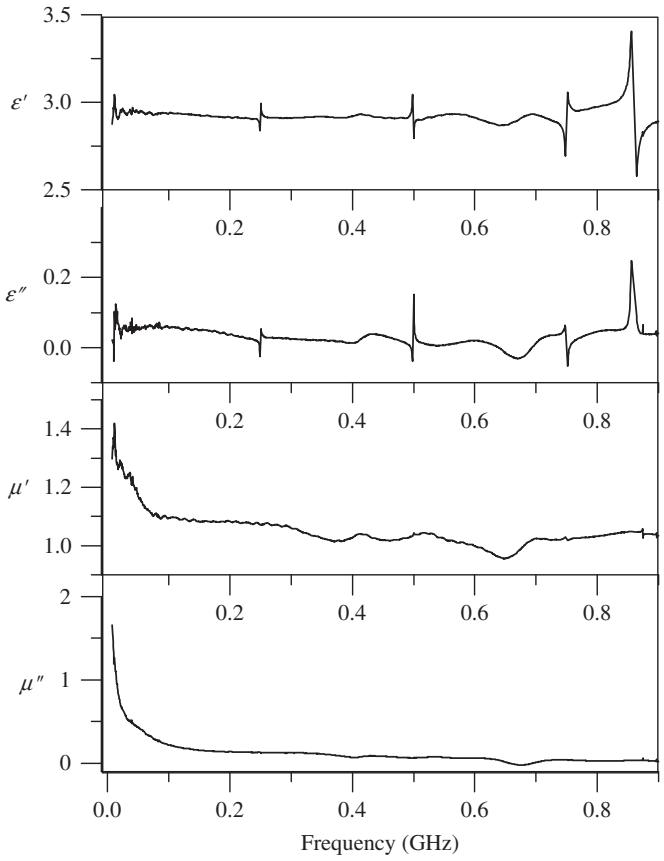

Fig. 7. Frequency variation of dielectric permittivity and magnetic permeability spectra of the $Ba_4Cu_2Fe_{36}O_{60}$ based composites.

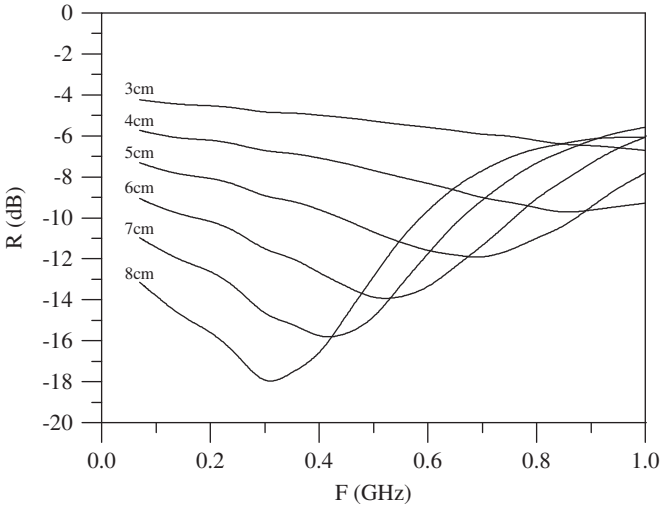

Fig. 8. Reflection loss spectra for the $Ba_4Co_2Fe_{36}O_{60}$ based composites.

dielectric loss factor (ε'') decreases with increasing frequency [16,17]. Both real part of magnetic permeability (μ') and magnetic loss factor (μ'') decrease with increase of frequency.

Figs. 8, 9 and 10 depict the microwave absorbing properties of the U-type hexaferrite composites U-Co, U-Ni and U-Cu respectively. U-Co composites demonstrated the highest microwave absorbing properties (~98%) and are tunable by manipulating the sample thickness. The least values of microwave absorption properties are observed for U-Cu composites. This is probably due to the highest magnetic loss factor in them.

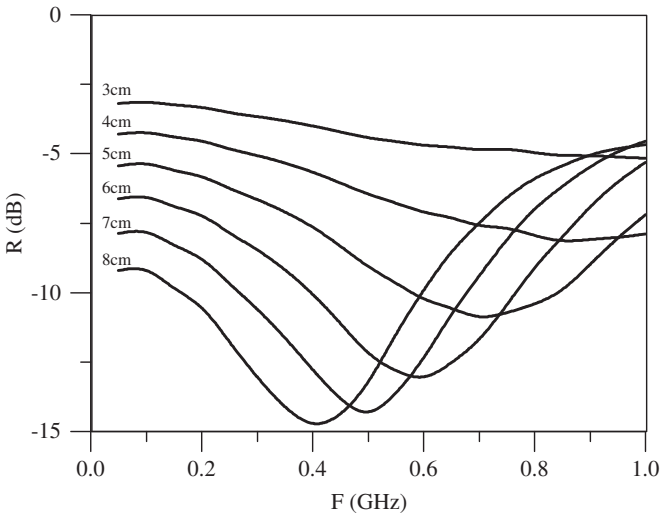

Fig. 9. Reflection loss spectra for the $Ba_4Ni_2Fe_{36}O_{60}$ based composites.

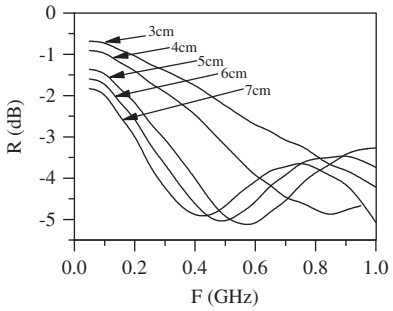

Fig. 10. Reflection loss spectra for the $Ba_4Cu_2Fe_{36}O_{60}$ based composites.

4. Conclusions

The U-type hexaferrites were synthesized using a modified solid state reaction technique. The composite has been prepared using polyethylene as a matrix with the U-type hexaferrite fillers with 60 wt% filler concentration. U-Co exhibits the maximum saturation magnetization value compared to the other two compounds. The decrease in saturation magnetization is very small between the temperatures 4 K and 50 K, monotonic between 50 K and 200 K and rapidly changing between 200 K and 300 K. The maximum magnetic inhomogeneity has been observed for U-Cu. Among the studied composites, Co based composites have the highest MW absorption (~98%) and are tunable; they shift toward lower frequency with increasing thickness of the sample.

References

[1] D. Lisjak, M. Drofenik, Journal of Magnetism and Magnetic Materials 272 (2004) E1817–E1819.
[2] D. Lisjak, D. Makovec, M. Drofenik, Journal of Materials Research 19 (2011) 2462.
[3] R.S. Meena, S. Bhattachrya, R. Chatterjee, Materials & Design 31 (2010) 3220.
[4] K. Okumura, T. Ishikura, M. Soda, T. Asaka, H. Nakamura, Y. Wakabayashi, T. Kimura, Applied Physics Letters 98 (2011) 212504.
[5] R.S. Meena, S. Bhattachrya, R. Chatterjee, Journal of Magnetism and Magnetic Materials 322 (2010) 1923.
[6] R.S. Meena, S. Bhattachrya, R. Chatterjee, Materials Science and Engineering B 171 (2010) 133.
[7] R.C. Pullar, A.K. Bhattacharya, Journal of Materials Science 36 (2001) 4805.
[8] V. Panwar, R.M. Mehra, J.O. Park, S.H. Park, Journal of Applied Polymer Science 125 (2012) E610.
[9] D.D.L. Chung, Carbon 39 (2001) 279.
[10] L. Liu, L.B. Kong, W.Y. Yin, IEEE Transactions on Electromagnetic Compatibility 53 (2011) 943.

[11] L. Liu, Z.H. Yang, L.B. Kong, P. Li, IEEE Transactions on Electromagnetic Compatibility 54 (2012) 88.
[12] S.R. Shannigrahi, K.P. Pramoda, F.A.A. Nugroho, Journal of Magnetism and Magnetic Materials 324 (2012) 140.
[13] C.K.I. Tan, K. Yao, J. Ma, Journal of the American Ceramic Society 94 (2011) 776.
[14] M.N. Afsar, D. Lisjak, A. Bahadoor, Y. Wang, IEEE Transactions on Magnetics 41 (2005) 3472.
[15] R.C. Pullar, A.K. Bhattacharya, Journal of Magnetism and Magnetic Materials 300 (2006) 490.
[16] A. Drmota, J. Koselj, M. Drofenik, A. Žnidaršič, Journal of Magnetism and Magnetic Materials 324 (2012) 1225.
[17] M.S. Boon, W.P.S. Saw, M. Mariatti, Journal of Magnetism and Magnetic Materials 324 (2012) 755.